Authors

Highly efficient reverse engineering process based on photogrammetry and NURBS in digitalisation of ship hull models

Paweł Bielski

Institute of Naval Architecture and Ocean Engineering, Gdańsk University of Technology, Poland

pawbiels@pg.edu.pl

Hanna Pruszko

Institute of Naval Architecture and Ocean Engineering, Gdańsk University of Technology, Poland

hanprus1@pg.edu.pl

Maciej Reichel
Corresponding Author

Ship Handling Research and Training Centre, Iława, Poland

Institute of Naval Architecture and Ocean Engineering, Gdańsk University of Technology, Poland

maciej.reichel@pg.edu.pl

Zbigniew Macikowski

Institute of Naval Architecture and Ocean Engineering, Gdańsk University of Technology, Poland

zbigniew.macikowski@pg.edu.pl

Preprint not peer reviewed

This preprint research paper has not been peer reviewed. Electronic copy available at: https://ssrn.com/abstract=4132953

Highly efficient reverse engineering process based on photogrammetry and NURBS in digitalisation of ship hull models

ARTICLE INFO

Keywords:
photogrammetry
shape measurement
reverse engineering
low cost
retrofitting
ship hull

ABSTRACT

We employed a low-cost photogrammetry procedure to capture the geometry of a manned ship model's prototype twin-skeg stern. Then, we replaced the original single-screw aft part in the current geometrical model with the measured part. The objective was to deliver the geometrical data in the form of the existing ship documentation, i.e. the lines plan. The measured hull was a manned model used at the Ship Handling Research and Training Centre in Iława, Poland. We used photogrammetric Agisoft Metashape software and Rhinoceros to create a NURBS-based lines plan of the stern. Then, satisfying the continuity and smoothness conditions, we integrated the prototype stern into the existing model. The described method is low-cost, reproducible, and time-efficient. One person can complete all the measurements and processing within several working days. Although we utilised a specific software set, multiple alternatives are possible. The obtained data is compatible with the standard lines plan.

Introduction

Aim and scope

The main goal of the presented investigation is to build a geometric representation of an existing ship model based on the actual measurements of its shape. The study is motivated by the need to test various possible modifications of hull geometry and propulsion-steering system for future improvements. For this purpose, we aim to perform numerical analyses and towing tank experiments. However, a precise geometric representation is needed beforehand to create the numerical and physical models.

In engineering, it is often helpful to perform multi-scale model investigations. Various scales allow running different types of experimental tests. Although scale-dependent effects are usually an issue, there are numerous approaches to overcome this obstacle Niklas and Pruszko (2019). In this study, we will focus on obtaining a geometry from a particular scale with the purpose of testing and exploitation in different scales. We will refer to these scales as:

- Full-scale ship (1:1). The actual vessel in its as-built form. It is the default scale to perform the majority of CFD calculations,
- Large-scale ship model (1:24). The physical model at the Iława Ship Handling Research and Training Centre for manoeuvre training purposes. It is the actual object measured during the study,
- Small-scale ship model (around 1:40). To be used in the towing tank experiments, such as resistance, propulsion, and cavitation tests.

ORCID(s):

Preprint not peer reviewed
This preprint research paper has not been peer reviewed. Electronic copy available at: https://ssrn.com/abstract=4132953

The task presented in this study is a part of a larger research project called twin-crp-pod ULCS. The project aims to evaluate the hydromechanical properties of a proposed ship with innovative hybrid steering-propulsion arrangement including contra rotating shaft and pod propellers in twin-screw version. The intended research covers towing tank experimental testing (small-scale model) and numerical Computational Fluid Dynamics analysis. We must capture the exact geometry of the hull to create the 3D numerical model and the small-scale model. The task presented in the paper is to obtain this geometry from the existing large-scale ship model, which already serves as a part of training equipment at the Iława Ship Handling Research and Training Centre. The digitalised geometry should be suitable for subsequent modelling and manufacturing, so NURBS Rogers (2001); Hughes, Cottrell and Bazilevs (2005) of the hull is the preferred approach (Fig. 1).

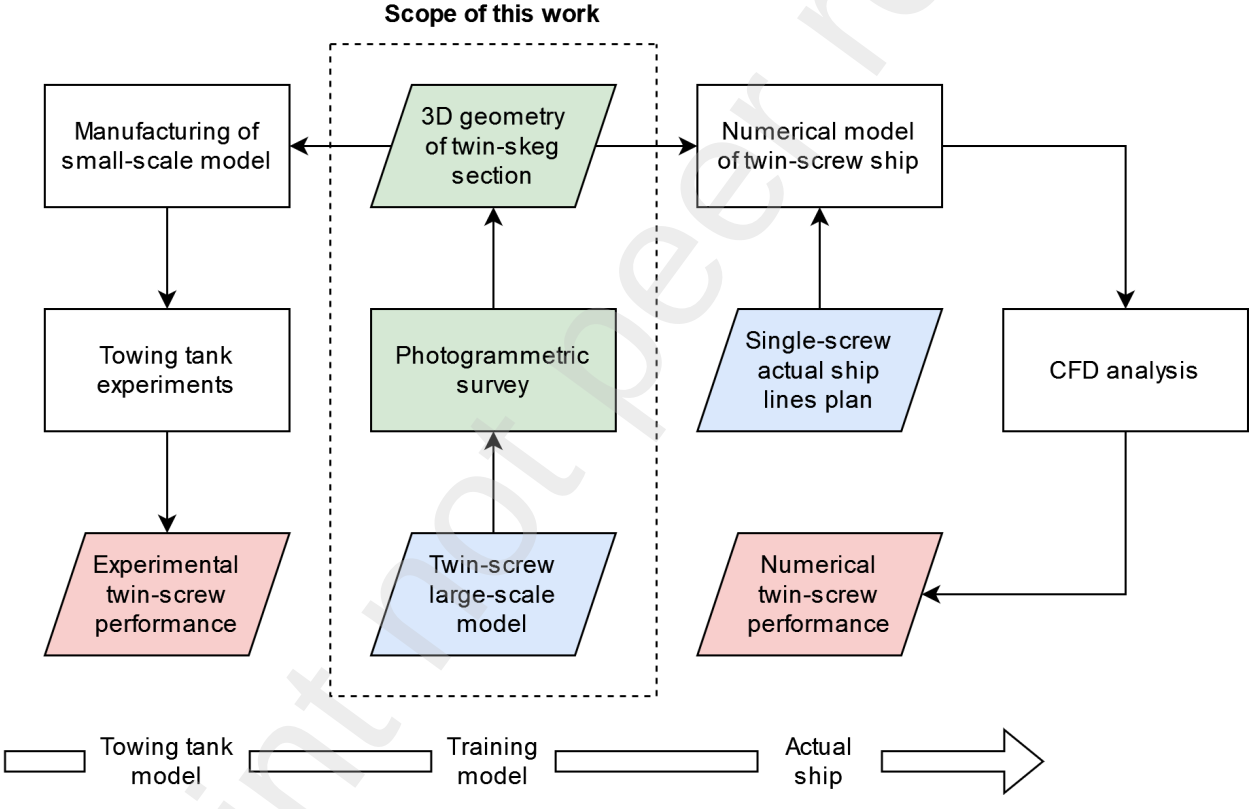

Figure 1: Flowchart of the larger project highlighting the part presented in the study

Background

The work presented in this paper is a part of the "twin-crp-pod ULCS" project funded through the ERA-NET MarTERA initiative. The project aims to apply three combined propulsion ideas to an Ultra Large Container Ship. These ideas are twin-screw arrangement, contra-rotating propellers and pod propulsion system. Each of them is well-established separately, although they rarely occur together. Some designs combine two of the mentioned solutions, e.g.

Preprint not peer reviewed
This preprint research paper has not been peer reviewed. Electronic copy available at: https://ssrn.com/abstract=4132953

hybrid crp-pod, where a single pod propulsor is placed behind a conventional propeller and works on the contra rotation principle Backlund and Kuuskoski (2000); ABB (2001); Ämmälä (2004); Sánchez-Caja, Pérez-Sobrino, Quereda, Nijland, Veikonheimo, González-Adalid, Saisto and Auriarte (2013). Most recent work on the single hybrid crp-pod propulsors focused mainly on numerical studies Wang, Xiong, Wang and Zhong (2016); He and Wan (2017); Zhang, Wu, Zhou, Cheng and Li (2019). For single crp-pod propulsion, there is considerable overall propulsive efficiency gain Wang, Min, Peng and Shen (2021). However, no reports exist on all three solutions combined in a single ship. Therefore, this project aims to investigate the whole life cycle of a twin-crp-pod ULCS, whether from a newbuilding or retrofitting starting point. The research analyses will include manoeuvring properties, general efficiency of the twin-crp-pod system and life cycle performance analyses from the cradle to the grave. Specific objectives that need evaluation to answer the main research question include:

- recognition of propulsion efficiency for a novel arrangement with the use of numerical methods and experimental investigation, including an assessment of the scale effect,
- identification of the manoeuvring abilities of redesigned ULCS that includes the verification of compliment with IMO requirements,
- definition of the technical and technological threats in the design, production, and exploitation stage,
- preparation of shipmasters and pilots for navigation and operation difficulties related to the novel propulsion system.

We must analyse multiple challenges related to the design of the ULCS twin-propeller configuration. The initial design study aims at a twin-screw twin-rudder arrangement and twin-crp-pod system for the new ship and the possibility to retrofit the twin-screw ship into twin-crp-pod propulsion. We need to prepare a new engine room arrangement and design of technical space from the propulsion and propulsion-related auxiliary machinery point of view. Comprehensive numerical analyses of flow around twin-propeller versions utilising CFD tools are also necessary. Therefore, the crucial task was to prepare high accuracy numerical and digital representations of the ship hull.

We selected an existing large-scale training model as a source for the reference geometry. The model contains a replaceable stern part to exchange the propulsion system on demand. During the study, two versions of the stern were available. The operating training model utilised a single-propeller hull version (Figure 2). The recently built twin-propeller stern was separated in a hall ashore.

The paper-based documentation of bow, midship and single-propeller stern sections offered an exact and faithful lines plan. The documentation was enough to create the digital representation of the geometry. In the case of the

Preprint not peer reviewed

This preprint research paper has not been peer reviewed. Electronic copy available at: https://ssrn.com/abstract=4132953

twin-propeller stern, we noticed considerable disparities between the design and actual form of the manufactured part. Therefore, we decided to capture the as-built geometry instead of relying on the documentation.

We opted to utilise photogrammetry to measure the geometry of the existing twin-skeg stern. The point cloud was then carefully converted to the lines plan similar to the available bow and midship documentation. Afterwards, these were combined and used to create a 3D NURBS digital surface model. The latter is the primary goal of the study described in this article.

Figure 2: Single-propeller single-rudder ULCS model during ship handling training

State-of-the-art

Koelman (2010) created an in-depth report regarding the measurement and re-engineering of existing ship hulls. He praised photogrammetry as a cheap and generally simple method, highlighting that it provides the processing human with topological information present in photographs. He also pointed out the limitations, such as space requirements, lighting conditions, landmarks placement and required skills of the user. One of his suggestions was to combine photogrammetry with terrestrial laser scanning. This approach has been extensively studied since that time. Shah, Gaggero, Gaiotti and Rizzo (2021) have used photogrammetry and its continuous recording counterpart, called videogrammetry or Structure from Motion (SfM), to survey the geometry of an existing ship. They have applied and described numerous pre-processing techniques which help achieve better results. They also discussed the main advantages of photogrammetry against laser scanning in surveying applications. Besides the rather obvious equipment costs, the most important advantage was the direct connection between the point cloud and the source image, which accelerates the visual identification of surveyed objects. Bartoš, Pukanská, Repáň, Kseňak and Sabová (2019) performed a threefold measurement of a racing vessel's surface. They used a traditional target-driven photogrammetric approach, a more modern Structure from Motion point cloud generation and the terrestrial laser scanning (TLS) technique. They evaluated each of these methods and found that the accuracy of photogrammetry is on par or even

Preprint not peer reviewed
This preprint research paper has not been peer reviewed. Electronic copy available at: https://ssrn.com/abstract=4132953

better than that of laser scanning. Besides the shape measurement, photogrammetry was also used in other ship-related applications, such as estimation of pitch and roll angles by Del Pizzo, Gaglione, Angrisano, Salvi and Troisi (2018).

Burdziakowski and Tysiac (2019) combined the two approaches and used photogrammetry and TLS as complementary tools to create a single point cloud of a submarine. Since the vessel was on the shore, its bottom parts were hardly accessible. It was also black, which amplified its light-absorbing properties. Photogrammetry proved to be an appropriate tool to capture most of the geometry, while TLS helped reach the inaccessible bottom areas of the ship. Abbas, Lichti, Chong, Setan, Majid, Lau, Idris and Ariff (2017) also paired photogrammetry with TLS to create a pre-calibration procedure for TLS. Interestingly, they treated the photogrammetric measurement as a benchmark for TLS, strengthening the image of photogrammetry as a precise and reliable tool. Biskup, Arias, Lorenzo and Armesto (2007) managed to measure the geometry of a 40 metres long ship hull using TLS. Although the precision was estimated to be around 10 mm, it is still considered sufficient for industrial surveying. Tang, Tang and Tay (2016) managed to measure as a similar-sized ship with double the precision using photogrammetry. However, targets needed to be manually placed on the hull surface. Paoli and Razionale (2012) integrated the optical measurement methods and robotics based on mechanical tracking. They created a highly automated system for scanning the freshly built yachts in the shipyard. Due to the stationary robotic arm support, the method included sewing several different point clouds created between respective device positions.

Wei, Ding, Huang, Yan, Huang and Leng (2019) have employed photogrammetry as a replacement tool for traditional measurements of ship blocks and ship sections. Hernández, Vaz, Cyrino and Alvarez (2019) used a similar technique to measure geometrical imperfections of ship panels. Woloszyk, Bielski, Garbatov and Mikulski (2021) applied photogrammetry to acquire initial deflections of stiffened plates for further experimental testing and numerical modelling for ultimate strength. Vorobyev, Garnier, van Dijk, Hagman and Gamstedt (2018) used laser scanning as a tool to measure displacements of a replica of the hull section during experimental loading. Chen, Garbatov and Guedes (2011) employed photogrammetry for quantification of the weld-induced deformation of ship components.

Yamafune, Torres and Castro (2017) and Calantropio, Chiabrando, Seymour, Kovacs, Lo and Rissolo (2020) have also discussed the influence of image pre-processing techniques on the quality of photogrammetric reconstruction. In this case, they performed underwater measurements of a sunken shipwreck. Image quality is of special interest in such limited lighting conditions. Prado, Gómez-Ballesteros, Cobo, Sánchez, Rodriguez-Basalo, Arrese and Rodríguez-Cobo (2019) presented an interesting approach by coupling the optical photogrammetric measurements with acoustic data to obtain a complete 3D shipwreck model. Costa and Guerra (2018) performed photogrammetric and laser scanning measurements to survey already extracted shipwrecks. By introducing a sophisticated calibration procedure, Menna, Nocerino, Del Pizzo, Ackermann and Scamardella (2011) managed to perform a quite different underwater

Preprint not peer reviewed

This preprint research paper has not been peer reviewed. Electronic copy available at: https://ssrn.com/abstract=4132953

photogrammetric measurement. They photographed the submerged part of a floating motorboat and recreated its shape using photogrammetry. This way, the docking operations were avoided.

Even though amateur cameras are often enough to get satisfying photogrammetric results, Lewis and Oswald (2019) stated that the software used is of significant importance. Agisoft Metashape proved to be a more precise tool than simple 3D scanning applications such as Qlone.

Our approach

For the sake of this study, we selected photogrammetry as the preferred method. Photogrammetry is generally cheaper and requires less specialised equipment than the TLS. A regular consumer-grade DSLR camera is usually enough for ground-based, medium-size objects to obtain acceptable results. There are, of course, sophisticated implementations of the technique, utilising UAVs, satellite or microscopic imaging, and others Ghosh (2005). However, this is not the case for our needs. Another great advantage of photogrammetry is scale independence, allowing for the reconstruction of individual particles and entire planets. It depends only on the resolution of source images, so everything captured by the camera sensor can be recreated. However, unlike the TLS or LiDAR, a bare-bones photogrammetric measurement can be carried out using limited equipment. Therefore we opted for photogrammetry during this study.

Among the limitations of the photogrammetric method are space requirements and lighting conditions. Generally speaking, it must be possible to take a clear shot. Images have to be proper in terms of photographic qualities. They need to be in-focus, well-lit, stationary and noise-free. These requirements put many constraints on the spatial arrangement of the measurement setup. The object must be easily accessible from each side; it should be lit by a stationary light with a fixed position against the object, and its surface should be devoid of any reflecting features. Because of these requirements, photogrammetry is not always the optimal surveying method. However, all of these conditions were met in our case.

Materials and Methods

Preparation of the object

The vessel of interest is a training model employed at the Ship Handling Research and Training Centre in Iława, Poland. The centre trains pilots in the handling of large ships and ships with unusual . The vessel selected for our study is a 1:24 model of 396 metres long ultra-large container ship. It currently operates with a single-screw single-rudder propulsion-steering arrangement. However, an alternative aft part is available. It has a twin-skeg geometry, allowing various propulsion systems. The segment is 5 metres long.

Preprint not peer reviewed

This preprint research paper has not been peer reviewed. Electronic copy available at: https://ssrn.com/abstract=4132953

We situated the object on its side to expose the underwater part for the measurements. It was located at the centre of a large warehouse to provide enough space around it to operate freely. We assured a distance of approximately 2 metres from each side to place the camera comfortably. We secured additional space to set up a scaffolding platform at a later stage of measurements. It was needed to take images of the hull side facing the roof in this configuration.

During photogrammetric measurements, any reflexes (Fig. 3) are undesirable because they alter the way the surface looks from different angles Agisoft LLC (2020). Since photogrammetry relies on the visual correlation of pixel groups (brightness and colour composition), it is crucial to maintain the features of a surface when the camera angle changes. Therefore, it is helpful to cover all reflective surfaces with an opaque layer. In our study, we covered the shiny surface of the hull with non-reflecting chalk paint (Fig. 4). The choice of chalk paint was motivated by three reasons. First – it is cheap and easy to distribute on the surface. Second – it creates a distinct texture on the surface, introducing additional contours and characteristics which further improve the photogrammetric correlation. It is especially beneficial with otherwise featureless surfaces, such as the considered hull. Third – chalk paint with water forms a suspension and not a solution. Therefore, it is easy to remove the layer from a smooth surface using plain water or water with soap after the measurement. Alternatively, we also tried to use ”artificial snow” in a spray for this purpose. We quickly discarded the idea because the substance did not cover the surface as efficiently as chalk paint. Its economic cost per surface area was also significantly higher, as was the process more time-consuming.

Figure 3: Light reflexes on the untreated surface of the vessel

Using Agisoft Metashape software, we generated ten circular 12-bit targets (markers) with a 10 mm diameter of central circles. We printed them on plain white paper and cut out the circles. After letting the paint dry for an hour, we placed the scaling markers on the hull surface. Since the hull was still damp and sticky after painting, glue was unnecessary. We fixed ten markers total, forming five pairs – one on the rear, three on the bottom and one on

Preprint not peer reviewed
This preprint research paper has not been peer reviewed. Electronic copy available at: https://ssrn.com/abstract=4132953

Camera	Canon EOS 50D
Lens	Canon EF 50 mm f/1.8 MkII
Focal length	50 mm
Image sensor	CMOS APS-C 22.3 x 14.9 mm
Crop factor	1.6
Sensor resolution	4752 x 3168 px
Pixel count	15 MPx

Table 1
Parameters of the camera and lens used for the study

the starboard side of the hull (Fig. 5). Agisoft Metashape software unequivocally identified each marker because of the coding. Photographs including the same coded targets automatically qualified as neighbours during the camera alignment. Each of the five pairs of targets had their relative distance manually measured in the real world with a tape measure. These distances later helped in scaling the model. This step is optional since the overall dimensions of the hull are known nevertheless. However, the inclusion of scaling markers introduces additional information to compute the uncertainty of the scaling factor.

Figure 4: Chalk paint creates a matte finish and reduces the reflexes

Image data acquisition

We used a single DSLR Canon EOS 50D camera equipped with a fixed Canon EF 50mm f/1.8 MkII lens (Tab. 1). We chose the lowest possible ISO value (ISO 100), a common practice in photogrammetric measurements Agisoft LLC (2020). To ensure a decent depth of field, we selected f/8.0 aperture. The camera operated in the aperture priority mode, so the shutter speed ranged from 1/25s to 1/2s depending on the local lighting conditions. We used a self-timer value of 2s to prevent any vibrations from manually triggering the release button since the exposure time was at times quite long.

The camera was attached to a stable tripod with adjustable height. Thus, the optical axis was always perpendicular to the measured surface when changing the camera's position. We used several external light sources apart from the

Preprint not peer reviewed

This preprint research paper has not been peer reviewed. Electronic copy available at: https://ssrn.com/abstract=4132953

natural light coming through the warehouse gate and the general lighting of the hall. Expressly, we set several pieces of floodlight to illuminate darker areas covered by the skeg. We chose to photograph only the starboard-side half of the hull due to the object's symmetry.

Figure 5: Measurement setup; An auxiliary camera shown at the left side of the image was not used during the study

The scheme and sequence of taking pictures maintained a constant 50% overlap between the photographs in vertical and horizontal directions (Fig. 6). Each region is present on at least four adjacent images. In the case of corners and edges of flat surfaces, the boundary photographs included the surrounding space (aside from the object) so that these corners and edges were also present in at least four different images. We took six transitional images around the corner between two surfaces meeting at a 90-degree angle, e.g. transom and side. Heavily curved and complex surfaces, such as the areas around the skeg, were treated individually. These regions were subjected to separate and more detailed procedures using additional photographs (Fig. 7).

The standard recommendation is to keep the angle between the optical axis of the camera and the measured surface around 90 degrees +/- 30 degrees. This way, the photographed area can approximately fit in the depth of field without defocusing and blurring. The resolution of the captured area must also be comparable to perform a pixel-based correlation. Thus, photographing at excessively sharp angles should be avoided. Irregular shapes like the skeg mentioned earlier require treatment with special care. We made sure that each region was visible and focused on multiple images by moving and rotating the camera above and below the skeg.

Preprint not peer reviewed

This preprint research paper has not been peer reviewed. Electronic copy available at: https://ssrn.com/abstract=4132953

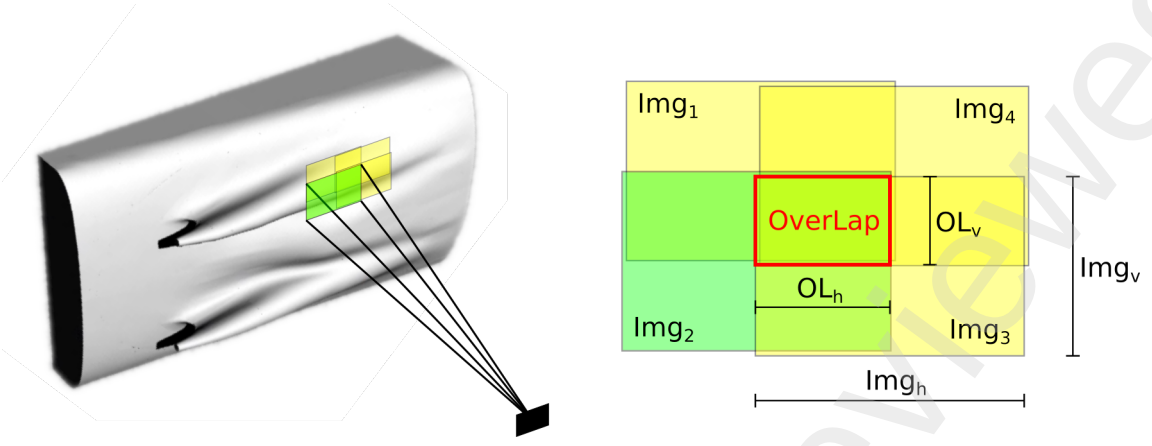

Figure 6: Overlapping of the neighbouring images is no lesser than 50% of the image dimensions

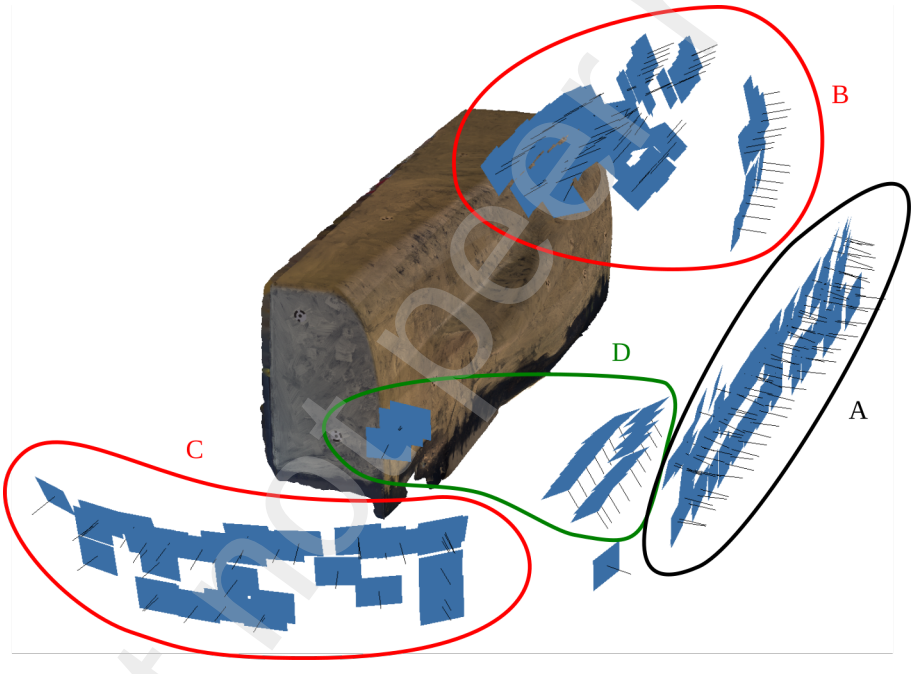

Figure 7: Positions of the acquired images relative to the object. The groups are used to reconstruct: A - bottom, B - transition from bottom to side, C - transition from bottom to transom, D - skeg.

Photogrammetric processing

After finishing the photographic task, we proceeded to the photogrammetric reconstruction. Each image was converted from the CR2 format to the TIFF format using open-source RawTherapee software. The only alteration applied to the image during the conversion was related to the lens distortion. We selected Profiled Lens Correction of Geometric Distortion and Vignetting based on the predefined Camera (Canon EOS 50D) and Lens (Canon EF 50mm f/1.8 MkII) profiles (capitalised are specific names of the RawTherapee settings and algorithms). Although this step is

Preprint not peer reviewed
This preprint research paper has not been peer reviewed. Electronic copy available at: https://ssrn.com/abstract=4132953

Software	Agisoft Metashape Professional 1.7.2
Operating system	Windows 10 64 bit
RAM	16 GB
CPU	Intel Xeon E3-1220 3.10 GHz
GPU	Quadro K620

Table 2
Software and hardware used for the photogrammetric processing

not recommended in the Agisoft Metashape manual, we have found that it helps to reduce the unwanted curvature of the reconstructed flat surfaces.

In the Agisoft software, all the images were loaded and masked. Only a portion of boundary photographs needed masking because most photographs presented the surface of interest in their entire area. We performed the camera alignment step using High-quality settings (original resolution), while dense cloud reconstruction and surfacing employed Medium settings (half resolution). We manually filtered the sparse and dense point clouds to remove the outliers and ran the camera re-alignment to update the calibration parameters (Optimize cameras). We selected the Average mode for texturing instead of the default Mosaic mode. This way, the apparent sharpness of the texture was used as a preliminary measure of precision because each region results from at least four image projections. Since the generated texture was indistinguishable from the source photographs, we accepted it is sufficiently sharp. Then, we proceeded to identify the scaling markers on the 3D textured model and set the previously measured distances as scale bars between the marker pairs. Having a low deviation between the scale bars, we assumed that the whole model was scaled correctly. Finally, the dense cloud was downsampled to 1 cm spacing and exported in the form of a text file.

Creation of the 3D model

We further processed the point cloud in the Rhinoceros software (Fig. 8). We have built a surface using an external MeshFromPoints script accessible as a plug-in in the Rhinoceros programme. This operation resulted in a polygon mesh (Fig. 9). The algorithm input data defined the spacing between adjacent points in the point cloud to obtain a robust model and good quality mesh. The resultant surface was manually checked, trimmed and compensated for any artefacts and discontinuities. It is also where we set the global coordinate system and rotated the model according to the principal directions. We extracted the hull lines by intersecting the model with equally spaced planes. This way, we obtained the resultant lines in the form of multi-node polylines. They were then manually transformed into smooth splines by interpolating the points of the polylines (Fig. 10). Finally, we used these splines to create NURBS surfaces. The criterion of the first derivative continuity condition (G0 and G1) governed each new surface using the edges of already existing surfaces and splines. This approach allowed us to obtain a smooth and complete surface model based on the photogrammetric measurements of the hull.

Preprint not peer reviewed

This preprint research paper has not been peer reviewed. Electronic copy available at: https://ssrn.com/abstract=4132953

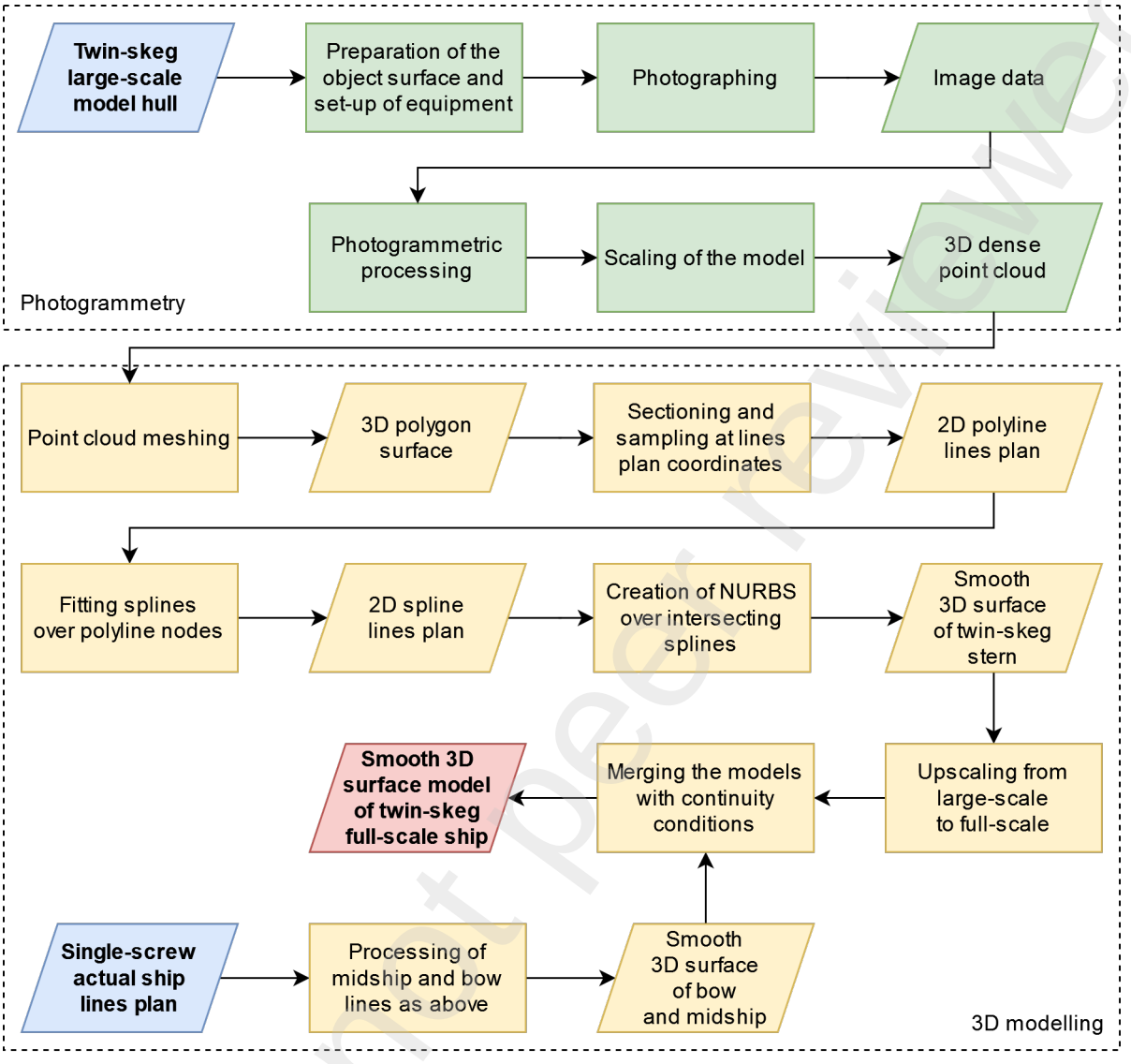
Twin-skeg large-scale model hull
Preparation of the object surface and set-up of equipment
Photographing
Image data
Photogrammetric processing
Scaling of the model
3D dense point cloud
Photogrammetry
Point cloud meshing
3D polygon surface
Sectioning and sampling at lines plan coordinates
2D polyline lines plan
Fitting splines over polyline nodes
2D spline lines plan
Creation of NURBS over intersecting splines
Smooth 3D surface of twin-skeg stern
Smooth 3D surface model of twin-skeg full-scale ship
Merging the models with continuity conditions
Upscaling from large-scale to full-scale
Single-screw actual ship lines plan
Processing of midship and bow lines as above
Smooth 3D surface of bow and midship
3D modelling

Figure 8: Flow chart of the procedure of digitalisation and merging the measured hull section with the existing model

Results and discussion

Photogrammetry

The measurement and processing were carried out within several hours, accounting for a single working day. Preparation of the surface (drying of the chalk paint included) took around 2 hours. Image acquisition took another 2 hours. We were sorting, pre-processing and masking the images for 1 hour. Photogrammetric processing, including the computation times of consecutive stages in Tab. 3, took another 1 hour. Total time did not exceed 8 hours.

We managed to achieve a satisfying average precision of 0.1 mm, given that the mean reprojection error was 0.6 px for a 0.15 mm/px resolution (Tab. 4). The total error significantly diminished by performing the repeated cycle of

Preprint not peer reviewed
This preprint research paper has not been peer reviewed. Electronic copy available at: https://ssrn.com/abstract=4132953

Figure 9: Effect of surfacing the downsampled point cloud in Rhinoceros software

Stage	Time	Quality	Parameters
Alignment	12:39	High	Filter points by mask
Depth maps	9:19	-	Aggressive depth filtering
Dense cloud	2:25	Low	
Surfacing	6:40	Low	
Texturing	4:40	-	Average blending mode
Total	35:43		

Table 3
Summary of the photogrammetric processing times (min:sec format)

Number of images	227
Number of tie points	182 000
Number of projections	820 000
Dense point cloud size	8 400 000
Number of surface polygons	562 000
Number of surface vertices	283 000
Downsampled point cloud size	128 000
Mean camera-to-object distance	1.82 m
Mean scale bars error	1.38 mm
Mean resolution	0.15 mm/px
RMS reprojection error	0.59 px
Max reprojection error	9.53 px
Mean key point size	4.08 px
File size	45 MB

Table 4
Statistics of the photogrammetric model

250 deleting the most uncertain tie points and optimising camera alignment. The maximum reprojection error in the model
251 was 9.5 px, which accounts for around 1.5 mm in the object scale. The distance between the scaling markers ranged
252 between 0.6 to 1.5 m, so the 1.4 mm average error accounts for a 0.1 to 0.2 % precision in physical dimensions. The
253 vast majority of pointwise reprojection errors are well below the pixel size (Fig. 11).

Preprint not peer reviewed
This preprint research paper has not been peer reviewed. Electronic copy available at: https://ssrn.com/abstract=4132953

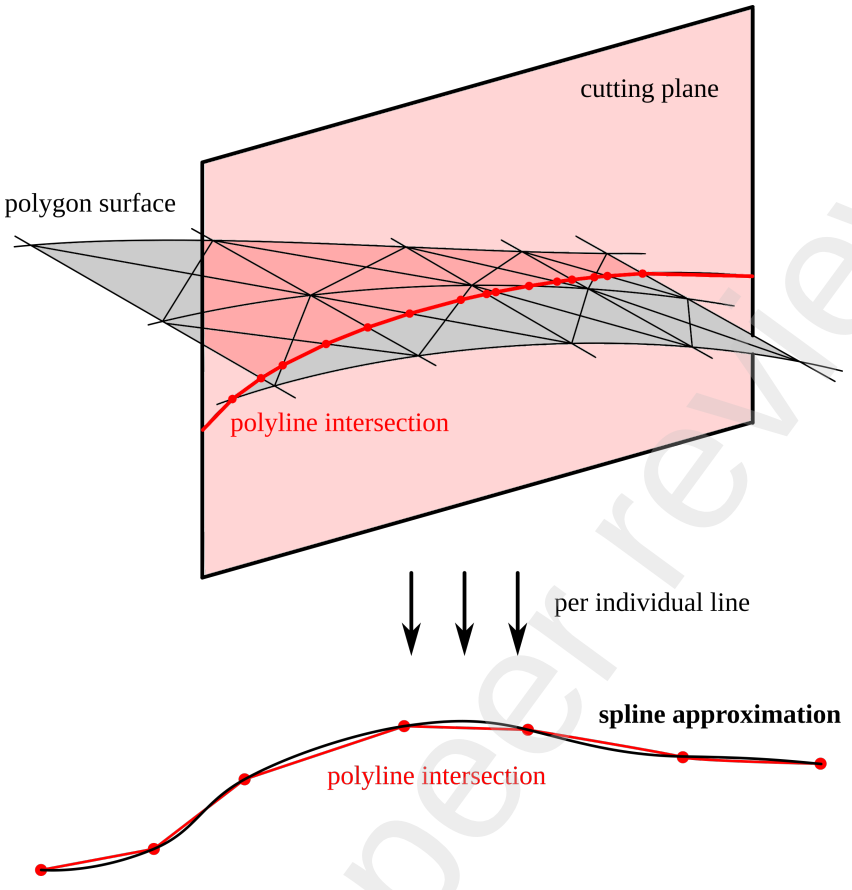

Figure 10: Visualisation of the procedure used to generate splines from surface intersections

We used the Adaptive Camera Model Fitting feature, which automatically computes the lens distortion parameters (related to decentration, radial and tangential distortion). The optimisation relies on minimising the mean reprojection error across all images. Since we used a single physical camera, there was a single set of distortion parameters for all images. Some reprojection residuals remain after fitting these parameters (again in a repeated cycle with deletion of underperforming tie points). Figure 12 presents these residuals in terms of location in the image area. The vast majority of the residuals indicate values well below a fraction of a pixel. It means that the general reprojection uncertainty stays at the sub-pixel level.

The image overlap of at least 50% in both directions worked out well. We maintained the technique across the whole area of interest. Figure 13 presents an example of the overlapping area across the four neighbouring images. The chalk pattern made this area much easier to identify for the human eye and the photogrammetric algorithm.

In most cases, the overlap was on the safe side, exceeding the assumed value of 50%. As a result, most areas were present in more than four photographs (mainly nine). However, the boundary photographs included the area of interest in a significantly decentralised position near the image's corners. It usually results in a more significant reprojection

Preprint not peer reviewed
This preprint research paper has not been peer reviewed. Electronic copy available at: https://ssrn.com/abstract=4132953

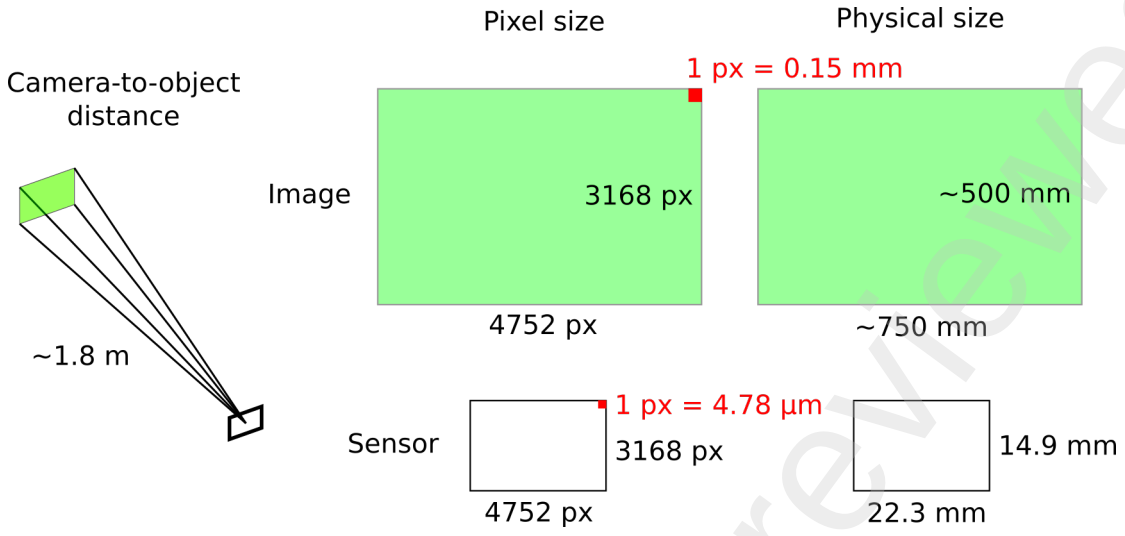

Figure 11: Relations between the physical dimensions and pixel size in the sensor and in the resulting image

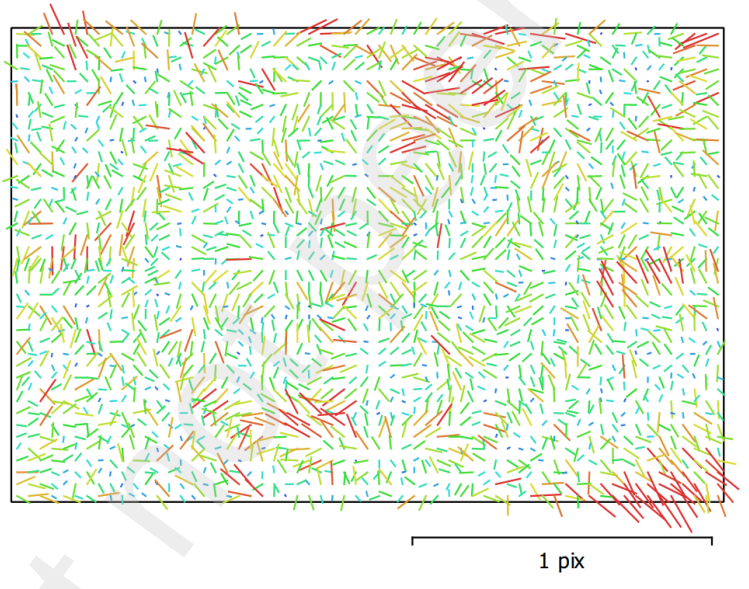

Figure 12: Mean reprojection residuals of the corrected lens distortion parameters at given sensor areas

uncertainty because lens distortion increases with the distance from the image centre. In our case, as can be seen in Figure 12, the reprojection residuals are small and relatively evenly distributed across the sensor. Thus, the whole image area is acceptable and valuable for reprojection.

The final model

We created the final model in three steps:

- The bow-midship part of the hull based on the already available lines plan (sections, buttocks and waterlines);

Preprint not peer reviewed
This preprint research paper has not been peer reviewed. Electronic copy available at: https://ssrn.com/abstract=4132953

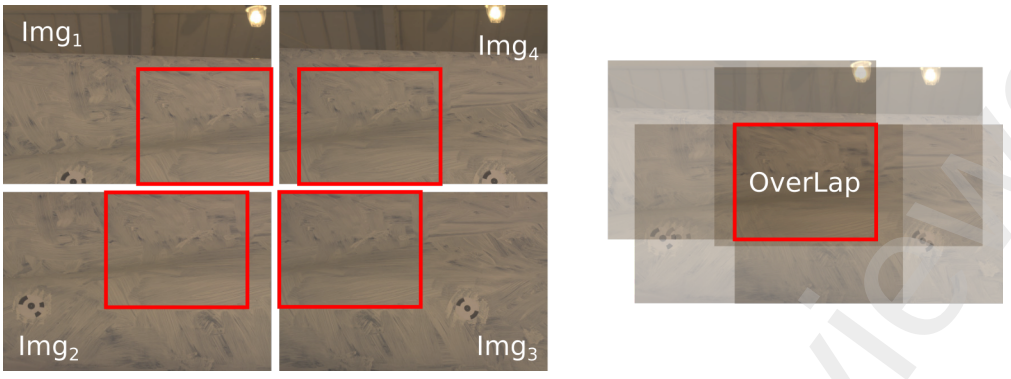

Figure 13: Example of the actual photographs overlapping in accordance with the shooting scheme

- The stern part of the ship based on the lines plan acquired through photogrammetry (Fig. 14);
- The final surface model is an effect of joining together the bow-midship with the stern (Fig. 15).

Firstly, we modelled the flat surfaces representing the deck, bottom and flat areas of the sides using Rhinoceros software. Then, we created the remaining surfaces based on the splines and edges of the existing flat areas. The splines came from smoothing the polylines generated from polygon mesh intersections with various cutting planes for the aft part. It is crucial since two sets of splines crossing each other are required to create the NURBS surface. Therefore, we generated the hull surface mainly from sections and waterlines or sections and buttocks. It results in a smooth, continuous, differentiable, and watertight surface (Fig. 16).

At this point, it is worth noting that surface fitting to the spline has its accuracy. Sometimes we needed to reduce this accuracy to ensure the smooth connection between the surfaces, i.e. the G0 and G1 conditions. However, it applied only to the most sophisticated areas of the hull, such as the bulbous bow and skegs. In the case of the polygon mesh built directly on the point cloud, the surface can have occasional holes and generally be discontinuous. It may also be impossible to enclose a volume within this surface. Any unnaturally sharp edges are unwanted since they can cause numerical hot spots in the consecutive Computational Fluid Dynamics analysis. Creating the surface based on splines in a parametric (analytical) form instead of polylines solves these problems. As an effect, we obtained a surface suitable for further CFD calculations (Fig. 15).

The main task was to reproduce the whole ship model with a hypothetical aft section and evaluate its hydrodynamic performance. To achieve this, we took the existing ship model and modified it to accommodate the new geometry. The original model was already available, so replacing it was a matter of simple operations in Rhinoceros. Thus, we created a complete model with a smooth surface based on the lines plan (both original and measured for the missing aft section).

Preprint not peer reviewed
This preprint research paper has not been peer reviewed. Electronic copy available at: https://ssrn.com/abstract=4132953

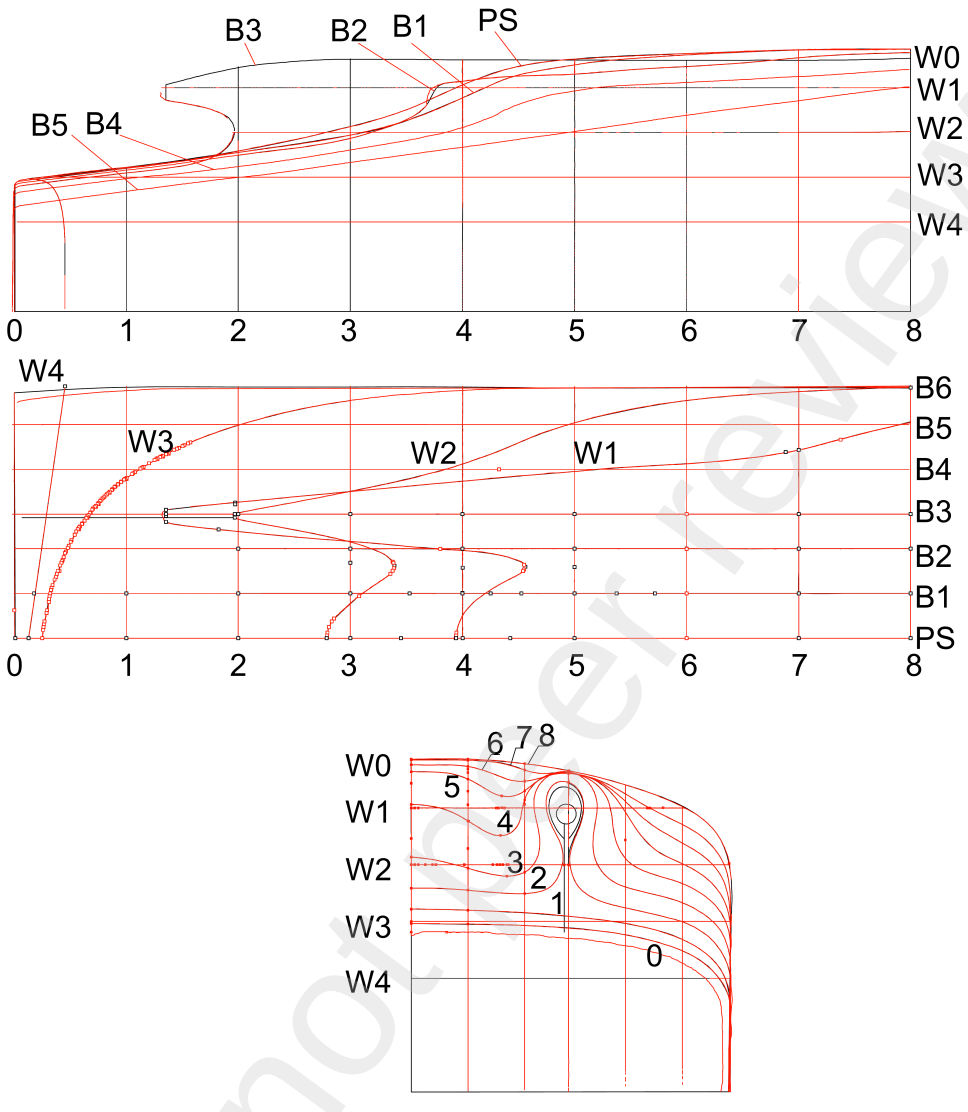

Figure 14: Section lines, buttock lines and waterlines created by intersecting the surface model with evenly distributed planes (red) and drawing splines around them (black)

Conclusions

We presented a fast and efficient way to measure and digitalise an existing part of the model ship for reverse engineering. The study consists of four main stages:

1. preparation of the surface and lighting,
2. photographing the hull,
3. processing the photographs into the point cloud,
4. further processing the point cloud to obtain the NURBS model of the entire hull.

Preprint not peer reviewed
This preprint research paper has not been peer reviewed. Electronic copy available at: https://ssrn.com/abstract=4132953

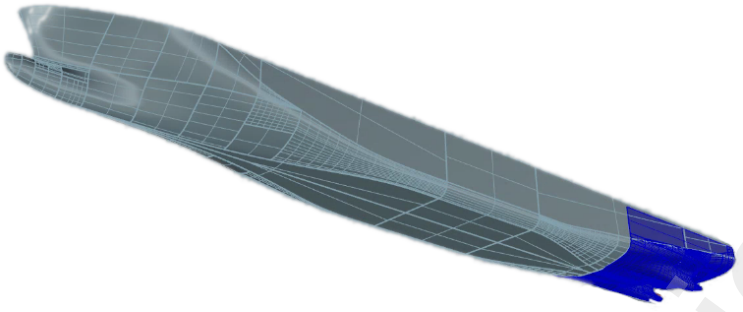

Figure 15: The measured aft section (blue) replacing the original section in the model of the full ship (gray)

Figure 16: The final model of the measured hull based on the lines plan created in Rhinoceros

Following this procedure, we created a high-quality model suitable for CFD calculations and designing a small-scale model for towing tank experiments. Based on our experience throughout the study, we formulated the following general remarks:

- chalk paint was more efficient, cheaper and provided better surface matting than ”artificial snow” in spray,
- completion of the model took three working days, where photogrammetric measurement and processing required one day and the creation of the NURBS model the next two days (for an experienced CAD user),
- both the camera/lens system and the computer were universal amateur-grade devices, eliminating the necessity to use specialised or expensive equipment,
- the achieved average precision of 0.1 mm was on-par or better than that reported with the LiDAR technique,

Preprint not peer reviewed

This preprint research paper has not been peer reviewed. Electronic copy available at: https://ssrn.com/abstract=4132953

- a significant limitation of the method lies in the surface requirements; since it must be non-reflecting, covering vast areas with a matting medium might be at times troublesome,
- however, many surface types (e.g. slightly corroded) are already adequate for the measurement without additional covering,
- the MeshFromPoints algorithm available as a Rhinoceros plug-in was robust and suitable for our needs,
- the G0 and G1 continuity conditions and accuracy reduction were necessary to ensure a smooth NURBS connection between the highly curved areas of the hull surface.

We consider this stage of the twin-cpr-pod ULCS project complete. Further investigation of the propulsion system efficiency will utilise the obtained hull form.

References

ABB, 2001. The CRP Azipod Propulsion Concept: The most economic way from crane to crane. Technical Report.

Abbas, M.A., Lichti, D.D., Chong, A.K., Setan, H., Majid, Z., Lau, C.L., Idris, K.M., Ariff, M.F.M., 2017. Improvements to the accuracy of prototype ship models measurement method using terrestrial laser scanner. Measurement: Journal of the International Measurement Confederation 100, 301–310. URL: http://dx.doi.org/10.1016/j.measurement.2016.12.053, doi:10.1016/j.measurement.2016.12.053.

Agisoft LLC, 2020. Agisoft Metashape User Manual. Agisoft Metashape , 160URL: https://www.agisoft.com/pdf/metashape-pro_1_5_en.pdf.

Ämmälä, P., 2004. CRP Azipod Propulsion Concept-Advanced Cost-Effective Solution. Journal of The Japan Institute of Marine Engineering 39, 544–554. URL: http://www.jstage.jst.go.jp/article/jime2001/39/9/39_9_544/_article, doi:10.5988/jime.39.544.

Backlund, A., Kuuskoski, J., 2000. The Contra Rotating Propeller (CRP) Concept with a Podded Drive, in: Motor Ship Conference, Amsterdam.

Bartoš, K., Pukanská, K., Repáň, P., Kseňak, L., Sabová, J., 2019. Modelling the surface of racing vessel's hull by laser scanning and digital photogrammetry. Remote Sensing 11. doi:10.3390/rs11131526.

Biskup, K., Arias, P., Lorenzo, H., Armesto, J., 2007. Application of terrestrial laser scanning for shipbuilding. IAPRS Workshop on Laser Scanning , 56–61URL: http://scholar.google.com/scholar?hl=en&btnG=Search&q=intitle:APPLICATION+OF+TERRESTRIAL+LASER+SCANNING+FOR+SHIPBUILDING#0.

Burdziakowski, P., Tysiac, P., 2019. Combined close range photogrammetry and terrestrial laser scanning for ship hull modelling. Geosciences (Switzerland) 9. doi:10.3390/geosciences9050242.

Calantropio, A., Chiabrando, F., Seymour, B., Kovacs, E., Lo, E., Rissolo, D., 2020. Image pre-processing strategies for enhancing photogrammetric 3D reconstruction of underwater shipwreck datasets. The International Archives of the Photogrammetry, Remote Sensing and Spatial Information Sciences XLIII-B2-2, 941–948. URL: https://www.int-arch-photogramm-remote-sens-spatial-inf-sci.net/XLIII-B2-2020/941/2020/, doi:10.5194/isprs-archives-XLIII-B2-2020-941-2020.

Chen, B.Q., Garbatov, Y., Guedes, C., 2011. Measurement of weld-induced deformations in three-dimensional structures based on photogrammetry technique. Journal of Ship Production 27, 51–62.

Costa, E., Guerra, F., 2018. 3D recording of ancient wooden boats for scientific and educational purposes. Applied Geomatics 10, 219–227. doi:10.1007/s12518-018-0228-0.

Preprint not peer reviewed

This preprint research paper has not been peer reviewed. Electronic copy available at: https://ssrn.com/abstract=4132953

Del Pizzo, S., Gaglione, S., Angrisano, A., Salvi, G., Troisi, S., 2018. Reliable vessel attitude estimation by wide angle camera. Measurement 127, 314–324. URL: https://linkinghub.elsevier.com/retrieve/pii/S0263224118304949, doi:10.1016/j.measurement.2018.05.104.

Ghosh, S.K., 2005. Fundamentals of Computational Photogrammetry. Concept Publishing Company.

He, D., Wan, D., 2017. Numerical investigation of open water performance of hybrid CRP podded propulsion system, in: The 8th International Conference on Computational Methods (ICCM2017), pp. 982–993.

Hernández, I.D., Vaz, M.A., Cyrino, J.C., Alvarez, N.M., 2019. Three-dimensional image-based approach for imperfect structures surface modeling. Journal of the Brazilian Society of Mechanical Sciences and Engineering 41. URL: http://link.springer.com/article/10.1007/s40430-019-1873-x?utm_source=researcher_app&utm_medium=referral&utm_campaign=RESR_MRKT_Researcher_inbound, doi:10.1007/s40430-019-1873-x.

Hughes, T.J., Cottrell, J.A., Bazilevs, Y., 2005. Isogeometric analysis: CAD, finite elements, NURBS, exact geometry and mesh refinement. Computer Methods in Applied Mechanics and Engineering 194, 4135–4195. doi:10.1016/j.cma.2004.10.008.

Koelman, H.J., 2010. Application of a photogrammetry-based system to measure and re-engineer ship hulls and ship parts: An industrial practices-based report. CAD Computer Aided Design 42, 731–743. URL: http://dx.doi.org/10.1016/j.cad.2010.02.005, doi:10.1016/j.cad.2010.02.005.

Lewis, M., Oswald, C., 2019. Can an inexpensive phone app compare to other methods when it comes to 3d digitization of ship models. The International Archives of the Photogrammetry, Remote Sensing and Spatial Information Sciences XLII-2/W10, 107–111. URL: https://www.int-arch-photogramm-remote-sens-spatial-inf-sci.net/XLII-2-W10/107/2019/, doi:10.5194/isprs-archives-XLII-2-W10-107-2019.

Menna, F., Nocerino, E., Del Pizzo, S., Ackermann, S., Scamardella, A., 2011. Underwater photogrammetry for 3D modeling of floating objects: The case study of a 19-foot motor boat. Sustainable Maritime Transportation and Exploitation of Sea Resources , 537–544.

Niklas, K., Pruszko, H., 2019. Full-scale CFD simulations for the determination of ship resistance as a rational, alternative method to towing tank experiments. Ocean Engineering 190, 106435. URL: https://doi.org/10.1016/j.oceaneng.2019.106435, doi:10.1016/j.oceaneng.2019.106435.

Paoli, A., Razionale, A.V., 2012. Large yacht hull measurement by integrating optical scanning with mechanical tracking-based methodologies. Robotics and Computer-Integrated Manufacturing 28, 592–601. URL: http://dx.doi.org/10.1016/j.rcim.2012.02.010, doi:10.1016/j.rcim.2012.02.010.

Prado, E., Gómez-Ballesteros, M., Cobo, A., Sánchez, F., Rodriguez-Basalo, A., Arrese, B., Rodríguez-Cobo, L., 2019. 3D modeling of Rio Miera wreck ship merging optical and multibeam high resolution points cloud. ISPRS Annals of the Photogrammetry, Remote Sensing and Spatial Information Sciences 42, 159–165. doi:10.5194/isprs-archives-XLII-2-W10-159-2019.

Rogers, D.F., 2001. An Introduction to NURBS With Historical Perspective. Elsevier. URL: https://linkinghub.elsevier.com/retrieve/pii/B9781558606692X50003, doi:10.1016/B978-1-55860-669-2.X5000-3.

Sánchez-Caja, A., Pérez-Sobrino, M., Quereda, R., Nijland, M., Veikonheimo, T., González-Adalid, J., Saisto, I., Auriarte, A., 2013. Combination of Pod, CLT and CRP Propulsion for Improving Ship Efficiency: the TRIPOD project, in: Third International Symposium on Marine Propulsors smp'13, pp. 347–357.

Shah, F.M., Gaggero, T., Gaiotti, M., Rizzo, C.M., 2021. Condition assessment of ship structure using robot assisted 3D-reconstruction. Ship Technology Research URL: https://www.tandfonline.com/doi/full/10.1080/09377255.2021.1872219?af=R&utm_source=researcher_app&utm_medium=referral&utm_campaign=RESR_MRKT_Researcher_inbound, doi:10.1080/09377255.

Preprint not peer reviewed

This preprint research paper has not been peer reviewed. Electronic copy available at: https://ssrn.com/abstract=4132953

2021.1872219.

Tang, C.H., Tang, H.E., Tay, P.K., 2016. Low cost digital close range photogrammetric measurement of an as-built anchor handling tug hull. Ocean Engineering 119, 67–74. URL: http://dx.doi.org/10.1016/j.oceaneng.2016.04.016, doi:10.1016/j.oceaneng.2016.04.016.

Vorobyev, A., Garnier, F., van Dijk, N.P., Hagman, O., Gamstedt, E.K., 2018. Evaluation of displacements by means of 3D laser scanning in a mechanically loaded replica of a hull section of the Vasa ship. Digital Applications in Archaeology and Cultural Heritage 11, 1–8. URL: https://doi.org/10.1016/j.daach.2018.e00085, doi:10.1016/j.daach.2018.e00085.

Wang, Z.z., Min, S.s., Peng, F., Shen, X.r., 2021. Comparison of self-propulsion performance between vessels with single-screw propulsion and hybrid contra-rotating podded propulsion. Ocean Engineering 232, 109095. URL: https://doi.org/10.1016/j.oceaneng.2021.109095, doi:10.1016/j.oceaneng.2021.109095.

Wang, Z.Z., Xiong, Y., Wang, R., Zhong, C.H., 2016. Numerical investigation of the scale effect of hydrodynamic performance of the hybrid CRP pod propulsion system. Applied Ocean Research 54, 26–38. URL: http://dx.doi.org/10.1016/j.apor.2015.10.006, doi:10.1016/j.apor.2015.10.006.

Wei, Y., Ding, Z., Huang, H., Yan, C., Huang, J., Leng, J., 2019. A non-contact measurement method of ship block using image-based 3D reconstruction technology. Ocean Engineering 178, 463–475. URL: https://www.sciencedirect.com/science/article/pii/S0029801819301118?dgcid=rss_sd_all, doi:10.1016/j.oceaneng.2019.03.015.

Woloszyk, K., Bielski, P.M., Garbatov, Y., Mikulski, T., 2021. Photogrammetry image-based approach for imperfect structure modelling and FE analysis. Ocean Engineering 223, 108665. URL: https://doi.org/10.1016/j.oceaneng.2021.108665https://linkinghub.elsevier.com/retrieve/pii/S0029801821001001, doi:10.1016/j.oceaneng.2021.108665.

Yamafune, K., Torres, R., Castro, F., 2017. Multi-Image Photogrammetry to Record and Reconstruct Underwater Shipwreck Sites. Journal of Archaeological Method and Theory 24, 703–725. URL: http://dx.doi.org/10.1007/s10816-016-9283-1http://link.springer.com/10.1007/s10816-016-9283-1, doi:10.1007/s10816-016-9283-1.

Zhang, Y.x., Wu, X.p., Zhou, Z.y., Cheng, X.k., Li, Y.l., 2019. A numerical study on the interaction between forward and aft propellers of hybrid CRP pod propulsion systems. Ocean Engineering 186, 106084. URL: https://doi.org/10.1016/j.oceaneng.2019.05.066, doi:10.1016/j.oceaneng.2019.05.066.

Preprint not peer reviewed

This preprint research paper has not been peer reviewed. Electronic copy available at: https://ssrn.com/abstract=4132953